

Optical transmission through circular hole arrays in optically thick metal films

L. Martín-Moreno

Departamento de Física de la Materia Condensada, ICMA-CSIC, Universidad de Zaragoza, 50009 Zaragoza, Spain

lm@unizar.es

F. J. García-Vidal

Departamento de Física Teórica de la Materia Condensada, Universidad Autónoma de Madrid, 28049 Madrid, Spain

fj.garcia@uam.es

Abstract: In this paper we extend our theoretical treatment of the extraordinary optical transmission through hole arrays to the case of circular holes and beyond the subwavelength limit. Universal curves for the optical transmission in different regimes of the geometrical parameters defining the array are presented. Finally, we further develop the statement by showing that extraordinary transmission phenomena should be expected for any system where transmission is through two localized modes, weakly coupled between them and coupled to a continuum.

© 2004 Optical Society of America

OCIS codes: (240.6680) Surface plasmons; (050.1220) Apertures

References and links

1. H. A. Bethe, "Theory of diffraction by small holes," *Phys. Rev.* **66**, 163 (1944).
2. A. Roberts, "Electromagnetic Theory of diffraction by a circular aperture in a thick, perfectly conducting screen," *J. Opt. Soc. Am. A* **4**, 1970 (1987).
3. T.W. Ebbesen, H.J. Lezec, H.F. Ghaemi, T. Thio, and P.A. Wolff, "Extraordinary optical transmission through sub-wavelength hole arrays," *Nature* **391**, 667-669 (1998).
4. L. Martín-Moreno, F.J. García-Vidal, H.J. Lezec, K.M. Pellerin, T.Thio, J.B. Pendry, and T.W. Ebbesen, "Theory of extraordinary optical transmission through subwavelength hole arrays," *Phys. Rev. Lett.* **86**, 1114-1117 (2001).
5. F.J. García-Vidal and L. Martín-Moreno, "Transmission and focusing of light in one-dimensional periodically nanostructured metals," *Phys. Rev. B* **66**, 155412 (2002).
6. E. Popov, M. Nevire, S. Enoch, and R. Reinisch, "Theory of light transmission through subwavelength periodic hole arrays," *Phys. Rev. B* **62**, 16100 (2000).
7. J.B. Pendry and A. MacKinnon, "Calculation of photon dispersion relations," *Phys. Rev. Lett.* **69**, 2772 (1992); P.M. Bell *et al.*, *Comp. Phys. Commun.* **85**, 306 (1995).
8. In the Fourier expansion formalism we are not aware of any published data on how convergency as a function of wavenumber cutoff is reached.
9. L.D.Landau, E.M. Lifshitz and L.P. Pitaevskii: *Electrodynamics of Continuous Media*, (Pergamon Press, Oxford, 1984).
10. P.M. Morse and H. Feshbach: *Methods of Theoretical Physics*, (McGraw-Hill, New York, 1953).
11. We take the dielectric constant for silver from: *Handbook of Optical Constants of Solids*, edited by E.D. Palik (Academic, Orlando, 1985).
12. J. Gomez-Rivas, C. Schotsch, P. Haring Bolivar, and H. Kurz, "Enhanced transmission of Thz radiation through subwavelength holes," *Phys. Rev. B* **68**, 201306 (2003).
13. F. Miyamaru and M. Hangyo, "Finite size effects of transmission property for metal hole arrays in subterahertz region," *Appl. Phys. Lett.* **84**, 2742 (2004).
14. H. Cao and A. Nahata, "Resonantly enhanced transmission of terahertz radiation through a periodic array of subwavelength apertures," *Opt. Express* **12**, 1004-1010 (2004).

15. M. Beruete, M. Sorrola, I. Campillo, J.S. Dolado, L. Martin-Moreno, J. Bravo-Abad, and F.J. Garcia-Vidal, "Enhanced millimeter wave transmission through subwavelength hole arrays," (Opt. Lett., in press).
 16. Q. Cao and P. Lalanne, "Negative role of surface plasmons in the transmission of metallic gratings with very narrow slits," Phys. Rev. Lett. **88**, 057403 (2002).
 17. W. L. Barnes, W. A. Murray, J. Dintinger, E. Devaux, and T. W. Ebbesen, "Surface plasmon polaritons and their role in the enhanced transmission of light through periodic arrays of subwavelength holes in a metal film," Phys. Rev. Lett. **92**, 107401 (2004).
 18. J.B. Pendry, L. Martin-Moreno and F.J. Garcia-Vidal, "Mimicking surface plasmons with structured surfaces," Science Express, 10.1126, 8 July 2004.
-

1. Introduction

Standard aperture theory states transmission of electromagnetic (EM) energy flux through a single hole in an otherwise opaque screen is, when the wavelength is much larger than the hole radius, much smaller than the energy flux impinging the hole area. Even when the screen thickness is negligible, the normalised-to-area transmittance scales as $(a/\lambda)^4$ [1], for $a \ll \lambda$ (a being the hole radius and λ the electromagnetic wavelength); considering the finite screen thickness further reduces the transmission [2] as, in the extreme subwavelength regime, all EM modes inside the hole are evanescent. This is why, six years ago, it came as a surprise the experimental finding [3] that the optical transmission through an array of subwavelength holes drilled in a metallic film could be orders of magnitude larger than what was expected for independent holes. Remarkably, this unexpected result appeared in a system (hole arrays) that had been extensively studied before for its interest as a selective filter. However, up to our knowledge, before Ebbesen's experiment all studies had concentrated on the transmission band-pass appearing in the regime $d < \lambda < \lambda_c$, where d is the array lattice parameter and λ_c is the cutoff wavelength for EM modes inside the hole. In this regime, the high-pass filtering is due to the hole EM cutoff, while the low-pass one is due to the energy redistribution that occurs when the first diffraction mode becomes propagating. A different mechanism must be responsible for the enhanced optical transmission (EOT) found by Ebbesen et al., which occurs for $\lambda_c < d < \lambda$. Already in [3] EOT was linked to the existence of surface plasmons in the air-metal interface. This was corroborated by a posterior theoretical study [4], which analyzed the way surface EM modes couple between themselves and to radiative modes, and how the coupled modes give rise to EOT. This theory was done, for analytical convenience, for a square array of square holes, within the surface impedance boundary condition approximation. In this paper we consider the case of infinite square arrays of circular holes. We show how a perfect metal approximation is able to capture the physics involved and, through a proper redefinition of the geometrical parameters defining the structure (in order to take into account the metal skin depth), even to provide a semi-quantitative estimation to the optical transmittance.

2. Theoretical formalism

The calculation of the optical properties of structured metal films is notoriously difficult from the computational point of view. This is due to the presence in the problem of very different length scales, as the lattice constant and the metal skin depth. Reliable calculations have been performed for systems with higher symmetry, as slits arrays [5]. Calculations in the fully three-dimensional case can be performed either by Fourier expansions [6] or through discrete versions of Maxwell equations in real-space [7]. Both methods require the introduction of cut-offs. At least in the real-space methodology, it is not trivial to assess whether convergency has been reached for computationally accessible values of the mesh parameter [8]. Furthermore, although exact solutions would be highly desirable (for instance for finding optimal geometrical parameters), extracting from them the physical mechanism responsible for the EOT may not be straightforward, something perhaps more easily achieved through approximate methods.

The theoretical formalism we use was presented in [4] for the case of an infinite array of square holes. In this section we briefly describe the approximations involved, and how to extend the formalism to the case of arrays of circular holes.

In our formalism, the dielectric constant of the metal (ϵ_M) is taken into account by considering surface impedance boundary conditions (SIBC) [9] on the metal-dielectric interfaces defining the metal film. The SIBC approximation takes into account both the penetration of EM field and absorption into the metal, being applicable when the skin depth in the metal is much smaller than all other length scales in the system. This is the case in this work, as all other length scales will be several hundreds of nanometers, while the skin depth for good metals in the optical regime is of the order of a few tens of nanometers. However, SIBC is not used in the metal walls defining the hole, in this case the metal is considered as a perfect conductor ($\epsilon_m = -\infty$). This approximation greatly simplifies the formalism, as the parallel components of the electric and magnetic wavefields inside the hole are related in a very simple way. Additionally, it allows the expression of the EM wavefield in terms of the eigenmodes of the hole which, for simple hole shapes (as rectangular or circular), are known analytically [10]. This approximation, therefore, neglects absorption by the metal walls surrounding the hole, something that is expected not to be a bad approximation, as the area of "horizontal" metal-dielectric interfaces is much larger than the area of "vertical" ones, for the typical geometries studied. More importantly, surrounding the hole by perfect conductor neglects the penetration of the EM fields in the metal "vertical" walls. This is a serious deficiency, as the optical transmittance is, in the subwavelength regime, very sensitive to the hole diameter. However, this deficiency can be circumvented by defining an (wavelength dependent) effective hole radius by adding to the geometrical radius a quantity proportional to the skin depth. The value of this quantity that best fits the experiments is not known and may be geometry dependent. Furthermore, depending on the preparation method, the dielectric constant at the hole walls may be different from the known bulk values. In this work we will not try to provide precise fits to experimental data and just take this proportionality factor equal to unity.

Within this approximation the calculation amounts to expanding the EM field in terms of the Bloch EM modes in each spatial region, and obtaining the expansion coefficients from matching the fields appropriately in all metal-dielectric interfaces. All that is needed therefore, are the EM modes in the vacuum region [9] and the hole waveguide. For circular holes the EM eigenmodes and their overlap with vacuum modes can be found for instance in [2].

3. Transmittance spectra

We consider an infinite square array of circular holes in a silver metal film, with lattice parameter $L = 750\text{nm}$, metal thickness $h = 320\text{nm}$ and hole diameter $d = 280\text{nm}$. These are typical experimental parameters in studies of EOT (the experimental transmission spectra, $T(\lambda)$, for a finite array of 21×21 holes can be found in Fig. 1 of [4]). The dielectric constant in all non-metallic regions is unity and the dielectric constant of silver is taken from [11]. Figure 1 shows the calculated $T(\lambda)$ (black curve). For each wavelength the effective hole diameter is taken as the nominal value plus twice the skin depth. Notice that, within the considered model, there are surface plasmons in the flat dielectric-metal interfaces (approximated by the SIBC) but there are no surface plasmons running along the surface of the hole. The cutoff wavelength in this case is $\lambda_c = 620\text{ nm}$, so the figure shows an EOT transmission peak at $\lambda \approx 780\text{ nm}$. The peak position is in reasonable agreement with the experimental data [4] (slightly enlarging the hole area provides a good agreement for both peak spectral position and area under the peak). However, the experimental peak height is never as high as in the calculation and the experimental peak is always wider, which could be indicative of the presence of disorder and/or finite size effects. Also shown in Fig. 1 (red curve) is the calculation for the same geometrical parameters

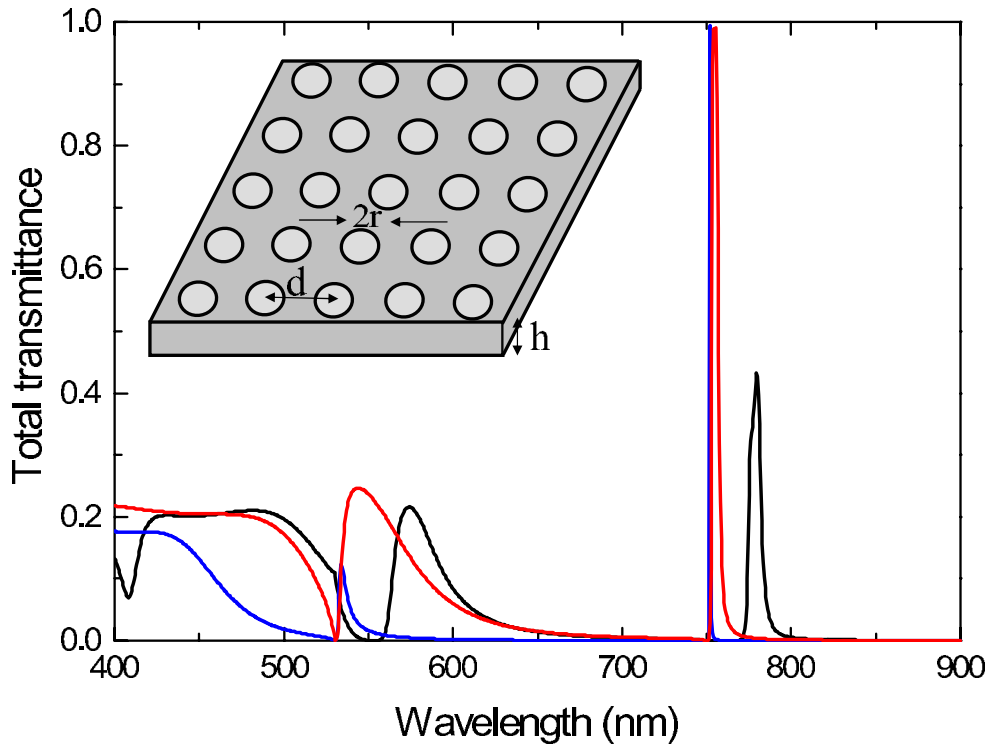


Fig. 1. Total transmittance spectra for a square array of circular holes of diameter $2r = 280\text{nm}$ perforated in a silver film of thickness $h = 320\text{nm}$. The period of the array is $d = 750\text{nm}$. Black curve shows our result imposing SIBC and considering an effective hole diameter (see text). Blue curve renders $T(\lambda)$ for the case in which silver is replaced by a perfect conductor and the red curve is an intermediate case in which perfect metal boundary conditions are assumed in the flat metallic interfaces but an effective hole diameter is considered.

and effective hole diameter, but considering $\epsilon_M = -\infty$ in the flat metal-dielectric interfaces. This last calculation shows that the effect of considering a realistic dielectric constant in the flat metal surface is to slightly red-shift the transmission. The calculation also shows that holes in a perfect conductor can also present EOT [4], although a flat interface between a dielectric and a perfect conductor does not support surface modes. Figure 1 (blue curve) also shows $T(\lambda)$ for the conditions of the red curve, but considering additionally that, in all the spectral range, the hole diameter equals its nominal value. The hole cutoff occurs now at $\lambda_c = 477\text{nm}$, but still a EOT peak appears. This time the peak position (much closer the condition $\lambda = d$, when the last diffraction order becomes non-propagating) and the area under the peak is very different from the experimental value.

Figure 2 shows the comparison between $T(\lambda)$ for arrays of circular holes (black curve here as in Fig. 1, repeated for visual convenience) and square holes. In the blue curve the nominal square side is 248nm , so that the squares have the same area as the circular holes (which also gives a similar propagation constant for the fundamental EM eigenmode inside both objects) whereas in the red curve the squares have a side equal to the diameter of the circular holes,

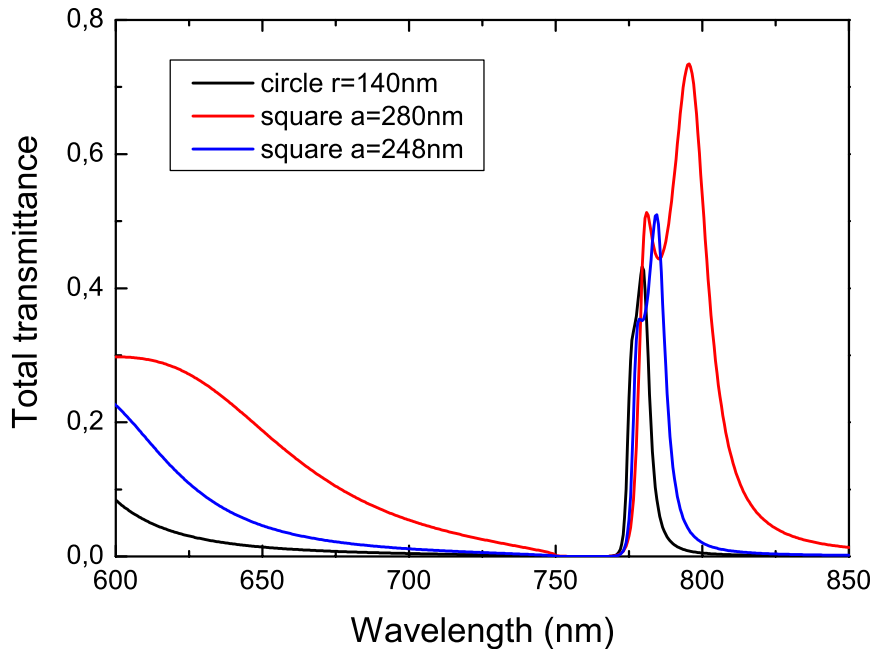


Fig. 2. Comparison between the transmission spectra of a square array of circular holes of diameter $2r = 280\text{nm}$ (black curve) with the corresponding ones of square array of square holes with two different sides: $a = 280\text{nm}$ (red curve) and $a = 248\text{nm}$ (blue curve).

280nm. In the square hole calculations an effective square side is also considered, adding to its nominal value twice the skin depth.

To summarize these results, EOT is present in the models considered, even appearing when the metal is considered to be a perfect conductor. This implies that EOT is also expected to appear in other frequency regimes where the perfect conductor approximation is even more justified (as for infrared, microwave and millimeter regimes), something that has been experimentally proven recently in a number of papers [12, 13, 14, 15]. If we consider the conductors as perfect, we can take advantage that Maxwell equations are scale-invariant. So, choosing the lattice parameter as the unit length, the transmittance spectra only depends on λ/d , a/d , and universal $T(\lambda)$ curves can be presented. Even in the optical regime, these curves serve as a guide to the different transmission regimes, if the skin depth is taken into account in the definition of an effective hole radius. Figure 3 renders $T(\lambda)$ within the perfect conductor approximation for a square array of circular holes, for $r/d = 0.1, 0.2, 0.3$ and 0.4 (panels 3(a), 3(b), 3(c) and 3(d), respectively) and for different values of a/h within each panel.

4. EOT and surface modes

In Ref. [4] we showed how EOT is related to the resonant excitation of surface EM modes appearing in the corrugated metal surface. However, some debate on this point can be found

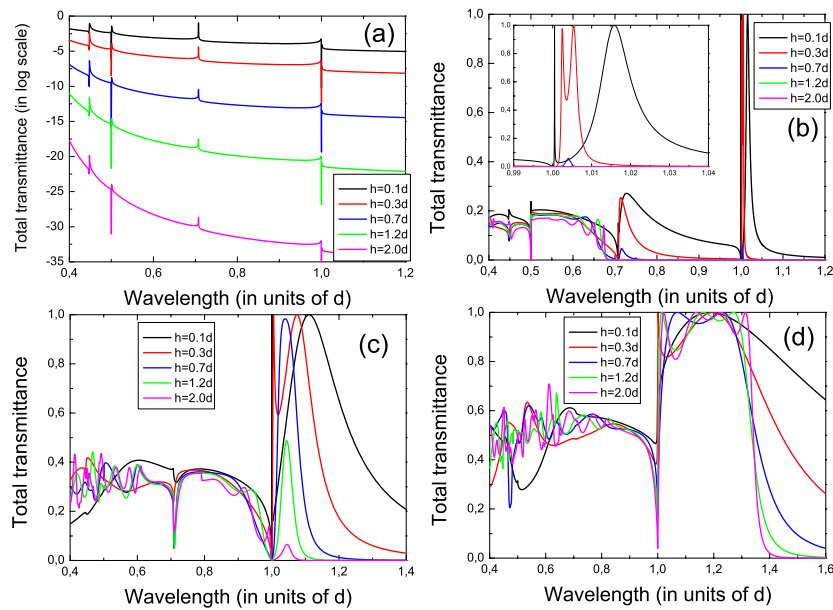


Fig. 3. Total transmittance spectra for different square arrays of circular holes perforated in perfect conductors. Panel (a) shows the case $r/d = 0.1$ for different values of the thickness h/d (note that the transmittance in this panel is shown in logarithmic scale). Panels (b), (c) and (d) analyze the cases $r/d = 0.2$, $r/d = 0.3$ and $r/d = 0.4$, respectively. In all cases the wavelength is expressed in units of the period of the array, d

in the literature. Another group explained EOT in terms of the existence of an (essentially) propagating mode inside the hole that appears in their calculations [6]. Surface states have even been considered as detrimental for the transmittance [16], due to their enhanced absorption; this has been proven wrong by recent experiments, which found that enhanced transmission and strong absorption occur at the same wavelength [17].

In this section we essentially repeat the line of reasoning presented in Ref. [4], this time for arrays of circular holes, and with slightly different approximations. We also present an analogy to a simpler (and perhaps better known system) that, in our opinion, makes our argument even more compelling.

The physical mechanism responsible for EOT can be more easily unveiled if the transmittance is calculated within the multiple scattering formalism. In this case, transmission amplitudes for crossing the whole system are obtained from the scattering amplitudes for crossing the different individual interfaces and the propagation constants of each EM eigenmode. In principle, these scattering amplitudes are matrices, involving the different eigenmodes inside the hole. However, only the fundamental (TE_{11}) eigenmode needs be considered given that it dominates the transmittance in the subwavelength regime. For normal incidence and $\lambda > d$,

$T(\lambda) = |t_0|^2$, where the zero-order transmission amplitude t_0 has the form:

$$t_0 = \frac{\tau^{12} \phi_P \tau^{23}}{1 - \rho^L \rho^R \phi_P^2} \quad (1)$$

here τ^{12}, τ^{23} are the transmission amplitudes for crossing the I-II and II-III interfaces, respectively. $\phi_P = \exp(ik_z h)$, $k_z = \sqrt{k^2 - (1.84/a)^2}$, k is the EM wavevector in vacuum, and ρ^L, ρ^R are the amplitudes for the TE_{11} mode to be reflected back into the hole at the II-I, II-III interfaces, respectively. In the system we are considering, where dielectric constants in reflection and transmission regions are equal, $\rho^L = \rho^R \equiv \rho$.

In Ref. [4] it was found that EOT peaks are associated to zeros in the denominator defining t_0 (actually, the spectral position is determined by $|\rho^L \rho^R \phi_P^2| = 1$), corresponding to constructive interference in the forward direction of all partial multiple scattered waves. In the subwavelength regime modes inside the hole are evanescent, so $|\phi_P^2| < 1$. If the reflection coefficient absolute value were restricted to values smaller than one, resonant denominators would not be possible. However, restriction on the values of reflection coefficients come from arguments based on current conservation which, for propagating modes imply $|\rho| < 1$, but for evanescent modes only forces $\text{Im}(\rho) > 0$, without posing any restriction on $|\rho|$. Figure 4 shows $\text{Re}(\rho)$ and $\text{Im}(\rho)$ as a function of wavelength, for an array of circular holes with $d = 750\text{nm}$, $h = 320\text{nm}$ and three different nominal hole radius. The calculation is done within the SIBC approximation, considering enough diffraction orders for achieving convergency. An even more simplified model was presented in Ref. [4], but we present here this version in order to show later the contribution of different effects. The real and imaginary parts of ρ clearly resembles the the form expected (from Kramers-Kronig relations) for a causal function in the vicinity of a localized mode. The finite width in the $\text{Im}(\rho)$ peak indicates that this localized mode is a resonance, i.e. it is coupled to a continuum into which EM energy is lost from the mode. This energy can be lost due both to absorption and radiative losses. In order to show the relative importance of this two mechanisms, we represent in the inset of Fig. 4 (green curve) the calculation for $r = 140\text{nm}$ within the SIBC but considering a hypothetical lossless silver. The comparison with the full calculation (inset of Fig. 4, red curve) shows that the resonant peak width, and therefore the typical time that the radiation stays at the surface, does not change much and is, within this range of geometrical parameters, limited by radiation losses. Up to this point, it could be thought that the surface modes are the bona fide surface plasmon polaritons of the flat silver surface which, due to the folding of their dispersion curve induced by the hole lattice can now couple to radiative modes. However, surface modes appear even in hole arrays within the perfect conductor approximation (inset of Fig.4, purple curve), although flat perfect conductor interfaces do not present surface plasmons polaritons. In Ref. [4] we termed these modes "surface plasmons of the corrugated metal surface", because they appear in metals, involve surface currents and, if the coupling to radiative modes is neglected, the EM wavefield is bound to the surface. However, this label may have created some confusion given that these modes appear even at corrugated *perfect* conductors. In order to further clarify the situation in this paper we have tried to avoid this (in our opinion minor) point, sticking to the terminology "surface EM modes". Recently, we have shown that the origin of these modes in corrugated perfect conductors come from the ability of these systems to spoof the response of a real electron plasma [18], which may have interesting applications for controlling light propagation in metal surfaces through geometry.

In this section, until now, we have discussed the existence of surface EM modes for a single interface. Even in an optically thick metal film, modes on both surfaces couple through the evanescent fields inside the holes, forming coupled surface modes that are now able to transfer energy efficiently through the system. The formation of the coupled surface EM modes is similar to, for instance, the formation of molecular levels from atomic levels. It was found in [4]

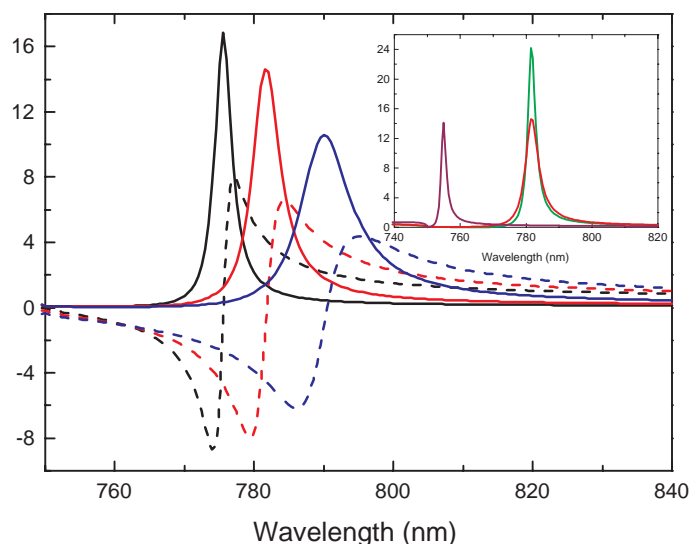


Fig. 4. Imaginary (full lines) and Real (dashed lines) parts of ρ (see text) for three different values of the hole radius: $r = 120\text{nm}$ (black curves), $r = 140\text{nm}$ (red curves) and $r = 160\text{nm}$ (blue curves). In the three cases, the period of the array d is 750nm . In the inset we compare the results for $\text{Im}(\rho)$ for the case $r = 140\text{nm}$ with different approximations to the dielectric constant of silver: real silver (red line), lossless silver (green line) and perfect conductor (purple line).

that, even if absorption is small, there are two transmission regimes depending on whether the time that the radiation stays at the surface before it is radiated (radiation time) is either larger or smaller than the time needed to form the "molecular" level (resonant time). In the former case calculations predict two large EOT peaks, whereas in the latter case, only one EOT peak appears, with height that decays exponentially as a function of h/a .

There is an analogy to a much simpler system, which can be easily worked out from beginning to end, that makes the previous argument even more compelling: consider the quantum mechanical (QM) transmission of a particle moving in one-dimension (1D) in the presence of the three-barrier potential depicted in Fig. 5. For simplicity consider all barriers of height $V = 30$ (in units of $\hbar = 1$, particle mass, $m = 1$), $L_1 = L_2 = 5$ and $W_1 = W_3 = 1$. Figure 5. shows the transmission probability as a function of the incident kinetic energy of the particle, for three different widths of the central barrier, W_2 . The transmission spectra for this system present the well known resonant tunnelling behavior (notice that $E < V$) through localized states in the wells formed between each two consecutive barriers. This system also shows the same transition, from a two transmission peaks to a one peak situation, as the transparency of the barrier separating both localized states in decreased. This 1D QM analog also serves to illustrate the properties of the reflection coefficient. Consider now that $W_2 \rightarrow \infty$. For a particle coming from $x = -\infty$, with $E > V$, the total reflection coefficient, r , must satisfy $|r| = 1$, due to current con-

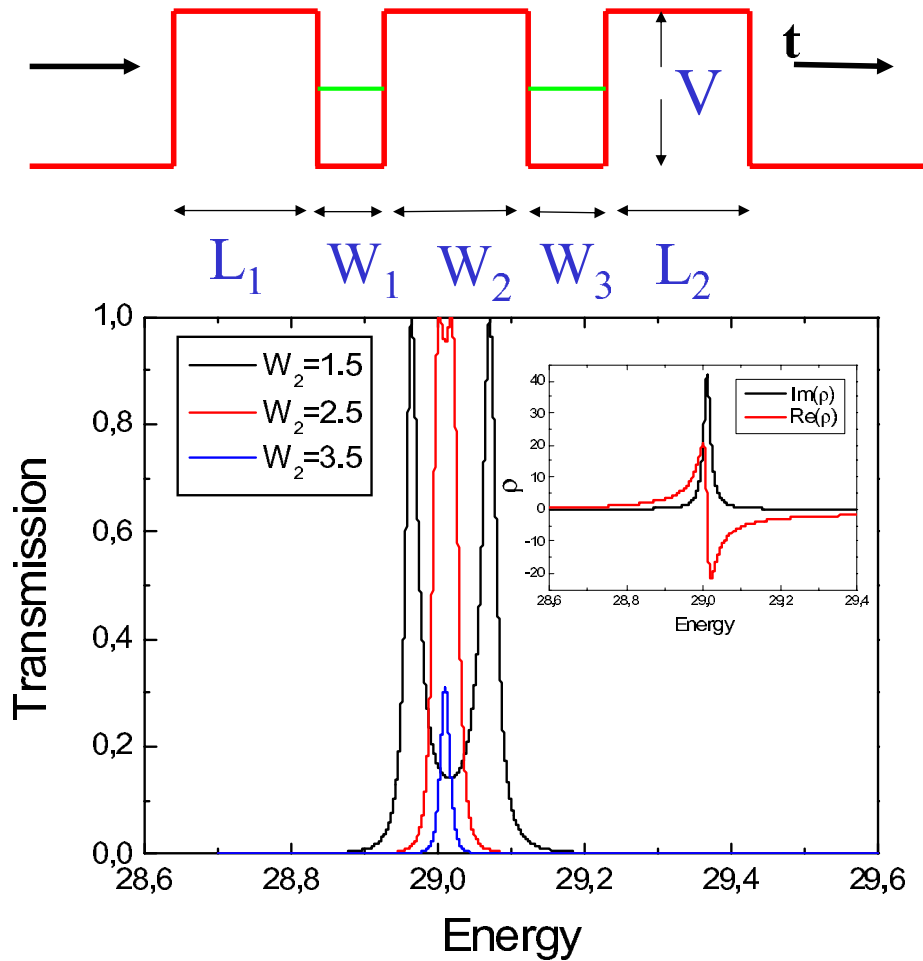


Fig. 5. Transmission versus energy spectra for the 1D QM analog depicted in the upper panel: a three-barrier potential of strengths $V = 30$ with geometrical parameters $L_1 = L_2 = 5$ and $W_1 = W_3 = 1$. Three cases with different intermediate barrier lengths W_2 are considered: $W_2 = 1.5$ (black curve), $W_2 = 2.5$ (red curve) and $W_2 = 3.5$ (blue curve).

servation. But, for $E < V$, the reflection amplitude for a wave at $x = L_1^-$ to be reflected back at $x = L_1^-$, ρ , is defined between evanescent modes and, as stated previously, current conservation only forces $\text{Im}\rho > 0$. Inset to Figure 5. shows that this is indeed the case, with the peak in $\text{Im}\rho$ marking the position of "leaky" (due to radiation) localized modes in the system.

5. Conclusions

In conclusion, we have analyzed theoretically the extraordinary optical transmission phenomenon observed in square arrays of circular holes perforated in optically thick silver films. We have also studied the appearance of this phenomenon in perforated perfect conductors and we have shown universal curves for the optical transmission as a function of the ratio between radii of the holes and period of the array for different metal thicknesses. We have ended by

establishing an analogy with a 1D quantum mechanical system: a particle crossing three consecutive barriers. We believe that this analogy further reinforces our statement that the physics of EOT is the physics of transmission through two localized states, weakly coupled between them and also coupled to a continuum.